THE JOURNAL OF PHYSICAL CHEMISTRY LETTERS
A JOURNAL OF THE AMERICAN CHEMICAL SOCIETY

pubs.acs.org/JPCL

Letter

Understanding the Effect of an Amorphous Surface on the Ultrafast Dynamics of a Heterogeneous Photoinduced Reaction: CD_3I Photoinduced Reaction on Amorphous Cerium Oxide Films

Md Afjal Khan Pathan, Aakash Gupta, and Mihai E. Vaida*

Cite This: *J. Phys. Chem. Lett.* 2022, 13, 9759–9765

Read Online

ACCESS | Metrics & More | Article Recommendations | Supporting Information

ABSTRACT: In this work, to understand how an amorphous surface influences the dynamics of surface photoinduced reactions, pump–probe spectroscopy in conjunction with mass spectrometry is employed to track the ultrafast evolution of intermediates and final products with time, mass, and energy resolution. As a model system, the photoinduced reaction of CD_3I adsorbed on amorphous cerium oxide films is investigated. A fraction of the first intermediates produced on a freshly prepared surface is trapped to passivate the surface. After the A-band excitation, the minimum dissociation time of CD_3I indicates that CD_3I adsorption geometries with either CD_3 or I facing the gas phase exist; however, the transient data suggest that most molecules are adsorbed with the I atom facing the surface. CD_3 and I are consumed to form I_2 and reform CD_3I, which are produced at a steady rate only after the intermediates have lost the excess translational energy released from photodissociation.

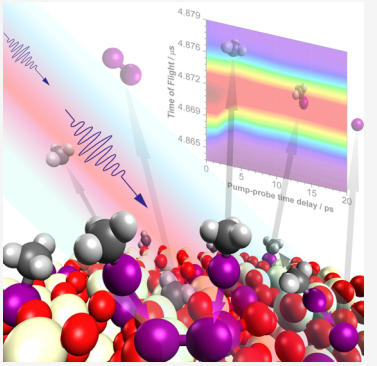

In surface-aligned reactions (SARs), reagent species produced by the photolysis of aligned molecules adsorbed on crystalline solids tend to move in well-defined directions relative to the crystal surface. In this case, the degrees of freedom of the surface chemical reactions are restricted, and therefore, the reaction dynamics and outcome are selected.[1,2] In contrast to SARs, on amorphous surfaces, molecules can have various adsorption geometries, and therefore, their reaction dynamics is unforeseeable. Amorphous materials have been widely employed as components of solid catalysts and involved in catalytic reactions with high industrial importance.[3] In general, amorphous surfaces have either higher activity or selectivity as compared to their crystalline counterparts.[4] However, there are many unknowns regarding the role that an amorphous surface plays in the reaction dynamics. The goal of this work is to gain detailed physical insights on how an amorphous surface, which presumably leads to random molecular adsorption geometries, affects the surface reaction. Therefore, the ultrafast photoinduced reaction dynamics of the deuterated methyl iodide (CD_3I) molecules adsorbed on amorphous cerium oxide films is investigated with time, mass, and energy resolution.

Cerium oxide is a reducible material that was employed in various catalytic applications.[5] Depending on its structure and oxidation state, cerium oxide can dramatically alter the adsorption and reactivity of various adsorbates.[6] Therefore, an amorphous cerium oxide surface should provide multiple adsorption sites that could lead to various molecular adsorption geometries. Methyl iodide is selected as a model system for photoinduced surface reaction investigations, because its gas-phase photodissociation has been studied both experimentally[7−13] and theoretically.[14−21] In addition, the gas-phase ultrafast photodissociation dynamics of methyl iodide has been also monitored in the femtosecond (fs) time domain.[22−26] The adsorption and the photoinduced reaction of methyl iodide were studied on crystalline metallic,[27,28] semiconducting,[29] and insulating surfaces[30−34] as well as on amorphous ice surfaces.[35,36] Furthermore, the ultrafast photoinduced reaction dynamics of methyl iodide was investigated on crystalline insulating films, which led to a prototypical example of so-called "Surface-Aligned Femtochemistry".[37−39]

All experiments presented in this work have been performed in an ultrahigh vacuum (UHV) surface science chamber equipped with various tools for surface preparation and characterization, which is presented in Section 1 of the Supporting Information. Details about the cerium oxide film synthesis and characterization are presented in Section 2 of the Supporting Information. The interaction of the CD_3I molecules with the cerium oxide surface is investigated via temperature-programmed desorption (TPD) and presented in Section 3 of the Supporting Information.

Received: July 24, 2022
Accepted: September 28, 2022
Published: October 13, 2022

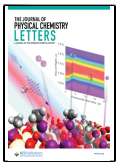

The ultrafast photoinduced reaction dynamics of CD_3I adsorbed on the amorphous cerium oxide surface is studied through the direct detection of intermediate species and final products using a technique that combines time-of-flight (TOF) mass spectrometry with laser spectroscopy and fast surface preparation with the molecules.[40] For the pump−probe mass spectrometry measurements, initially, CD_3I is continuously dosed ($<1 \times 10^{-8}$ Torr) on the cerium oxide surface using a UHV compatible gas inlet. The continuous admission of CD_3I is used to instantaneously replenish the molecules desorbed from the surface during the reaction. To restrict the amount of CD_3I molecules to submonolayer and maintain this coverage during the reaction, the sample temperature is kept at 160 K (see details in Section 3 of the Supporting Information). The sample is irradiated with the pump laser pulse (266 nm, 25 mW/cm^2, p-polarized) to excite the CD_3I molecules into the dissociative A-band, which leads to the formation of CD_3 and I neutral fragments. Subsequently, the probe laser pulse (266 nm, 300 mW/cm^2, p-polarized) is used to ionize the neutral fragments and reaction products that are formed at the surface. The ions are removed from the surface by a static electric field and analyzed by a time-of-flight mass spectrometer (TOF-MS).

Figure 1 shows a TOF mass spectrum of CD_3I recorded from a 10 monolayer (ML) thick cerium oxide film. Peaks

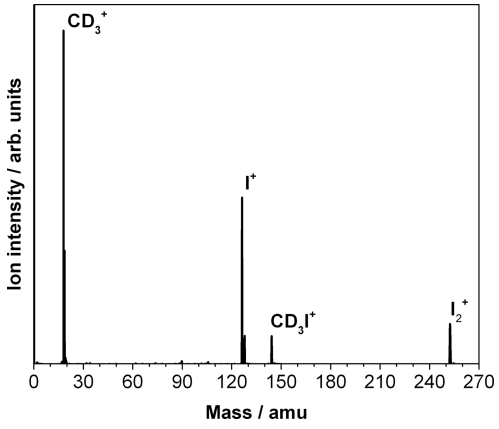

Figure 1. TOF mass spectrum obtained from CD_3I continuously dosed at a partial pressure of $\lesssim 1 \times 10^{-8}$ Torr on a 10 ML cerium oxide surface at a pump−probe time delay of 4 ps. The surface is kept at 160 K during the measurement to restrict the number of molecules at the surface. The spectrum is obtained by summing the mass signals over 1×10^6 laser shots.

corresponding to CD_3^+, I^+, I_2^+, and CD_3I^+ are detected. To demonstrate that the signal detected by the TOF-MS originates only from the surface and not from the gas phase, mass spectra of CD_3I at various surface temperatures are recorded while the CD_3I background pressure is kept at 1×10^{-8} Torr (see Figure S5). No signal is detected with TOF-MS when the surface temperature is raised above 263 K, corresponding to the temperature at which all physisorbed CD_3I molecules are desorbed from the cerium oxide surface, indicating that chemisorbed CD_3I molecules are neither desorbed from the surface nor detected during the surface photoinduced reactions.

Interestingly, when a mass spectrum is recorded from a freshly prepared cerium oxide surface at a fixed pump−probe time delay and a constant CD_3I background pressure, the rate

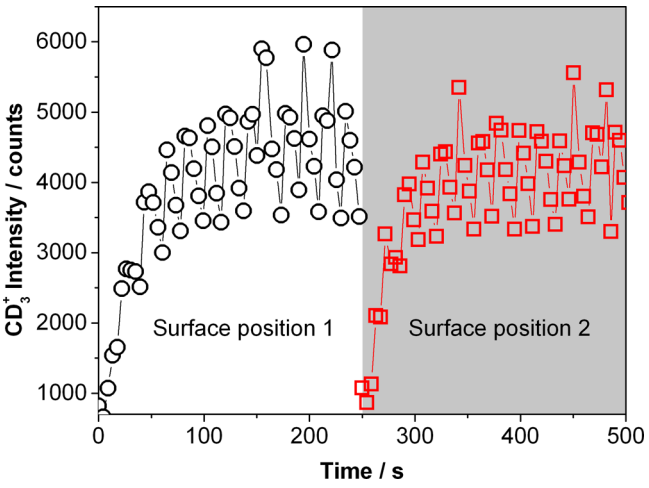

Figure 2. Time evolution of the CD_3^+ signal intensity after the initial irradiation of a cerium oxide film continuously dosed with CD_3I molecules $\left(P_{CD_3I} = 1 \times 10^{-8}\ \text{Torr}\right)$. After 250 s, the sample position is changed so that a new area of the cerium oxide film is irradiated by the laser (gray background). Each data point represents the CD_3^+ signal summed over 3000 laser shots. During the measurement, the surface temperature is kept at 160 K. The data is recorded at 25 mW/cm^2 with a 266 nm pump laser beam and 300 mW/cm^2 with a 266 nm probe laser beam at a pump−probe time delay of 1.5 ps.

at which the reaction products are detected increases within 100 s after the sample is first irradiated. Figure 2 shows the time evolution of the CD_3^+ signal intensity recorded from a freshly prepared cerium oxide film with CD_3I molecules in the first 250 s after the initial laser irradiation of the sample. After 250 s of laser irradiation, the sample position is changed so that a new area of the sample is irradiated. As can be seen in Figure 2, the CD_3^+ signal intensity gradually increases within the first 100 s and subsequently reaches a plateau. When the sample position is changed after 250 s, the CD_3^+ signal intensity drops to a similar value that was obtained on the first irradiated cerium oxide area immediately after the irradiation started. Subsequently, the CD_3^+ signal intensity gradually increases within 100 s and reaches a plateau again.

The trend of the CD_3^+ in Figure 2 cannot be attributed to an accumulation of CD_3I at the cerium oxide surface because (i) the amount of CD_3I molecules at the surface is kept constant by maintaining the surface temperature at 160 K and (ii) the CD_3^+ signal drops when the sample position is changed to a new cerium oxide area that was never irradiated by the laser. The signal observed in Figure 2 can be attributed to a passivation with CD_3 and I fragments of the surface reactive sites, presumably the low coordinated Ce atoms that are not occupied by chemisorbed CD_3I molecules. Therefore, immediately after the laser irradiation of a freshly prepared cerium oxide film with CD_3I molecules, a substantial number of fragments are trapped at the surface instead of being released into the gas phase. For the laser power used in this study, after about 100 s, the surface is passivated; i.e., the reactive sites are occupied. Additionally, CD_3^+ and I^+ fragments are produced and released into the gas phase at a steady rate. Hence, the appearance of the plateau in Figure 2 indicates that the surface is passivated.

The signal observed in Figure 2 cannot be attributed to damage or modification of the surface due to laser heating effects, because higher laser intensities have been employed in

https://doi.org/10.1021/acs.jpclett.2c02294
J. Phys. Chem. Lett. 2022, 13, 9759−9765

similar investigations on highly crystalline oxide surfaces and no similar trends have been observed.[37−42] Furthermore, a flash heating of the surface to 850 K is sufficient to remove the attached fragments, which leads to a surface that has the same properties and behaves as a newly prepared cerium oxide film. In addition, identical Auger and valence band photoemission spectra (not shown here) are recorded from the cerium oxide films before and after prolonged irradiation of the sample by the pump and probe laser beams. This indicates that the pump and probe laser pulses employed in this investigation do not change the composition and electronic structure of the sample, which rules out the possibility of sample damage by the laser radiation. On the basis of the low intensities of the iodine and carbon transitions detected in Auger electron spectroscopy from the irradiated samples (not shown here), we estimate that less than 20% of the surface is passivated with I and CD_3 fragments as well as chemisorbed methyl iodide molecules (see the TPD investigation in Section 3 of the Supporting Information).

To explore the temporal evolution of the intermediates and final products, the intensity of each mass peak displayed in Figure 1 is monitored as a function of the pump−probe time delay. Figure 3a shows the transient evolution of the CD_3^+ mass signal intensity, in which the open symbols represent the measured data obtained by summing the mass peak at 18 amu over 3000 laser shots at various pump−probe time delays. The transient signal consists of a sharp peak centered at a pump−probe time delay of 0 fs. Subsequently, the CD_3^+ signal rises, reaches a maximum at 650 fs, and finally decays. The sharp peak at zero-time delay (ZTD) is attributed to the interference of the pump and probe laser beams, which leads to a large increase in the laser intensity and hence a multiphoton excitation of the adsorbed CD_3I molecules into cationic dissociative states. The sharp peak at ZTD is identical to the autocorrelation curve obtained by monitoring the integral transient photoemission signal produced by both 266 nm pump and probe laser beams (not shown here). The full width at half-maximum (fwhm) of 103 ± 3 fs of the ZTD peak, which is obtained by a Gaussian fit, indicates a pulse duration of about 73 fs.[43] The best fit to the transient signal after ZTD by a model composed of a delayed exponential rise and exponential decay functions convoluted with the pump−probe autocorrelation function (red curve in Figure 3a) indicates that the CD_3^+ signal appears with a coherent delay (t_0) of 126 ± 20 fs, rises with a time constant (τ_{rise}) of 200 ± 20 fs, and decays with a time constant (τ_{decay}) of 2.5 ± 0.3 ps. The transient signal of I^+, which is displayed in Figure 3b, follows the same trend as the CD_3^+ signal. The I^+ transient consists of a low intensity peak centered at ZTD, followed by a rise that reaches the maximum intensity at 3.5 ps and a decay. The same fitting model used in Figure 3a indicates that I^+ appears with a coherent delay (t_0) of 126 ± 20 fs, rises with a time constant (τ_{rise}) of 1.4 ± 0.06 ps, and decays with a time constant (τ_{decay}) of 8.0 ± 0.3 ps.

Figure 3c displays the transient signal of I_2^+. No I_2^+ signal is detected until a pump−probe time delay of 880 fs. Subsequently, the signal rises and does not decay within the longest pump−probe time delay, i.e., 80 ps, employed in this study (not shown here). The best fit to the measured data, consisting of a delayed exponential rise function convoluted with the pump−probe autocorrelation function (cf. solid red curve in Figure 3c),[37] confirms that no I_2^+ signal is detected up to 880 ± 20 fs and provides the rise time constant of the I_2^+ signal, which is τ_{rise} = 8.5 ± 0.3 ps. Figure 3d displays the transient signal of CD_3I^+, which follows the same trend as the I_2^+ signal. The best fit to the measured data using the same model as in Figure 3c shows that no CD_3I^+ is detected up to 800 ± 100 fs. Subsequently, the CD_3I^+ transient signal rises with a time constant of 2.2 ± 0.3 ps and reaches a plateau at about 5 ps.

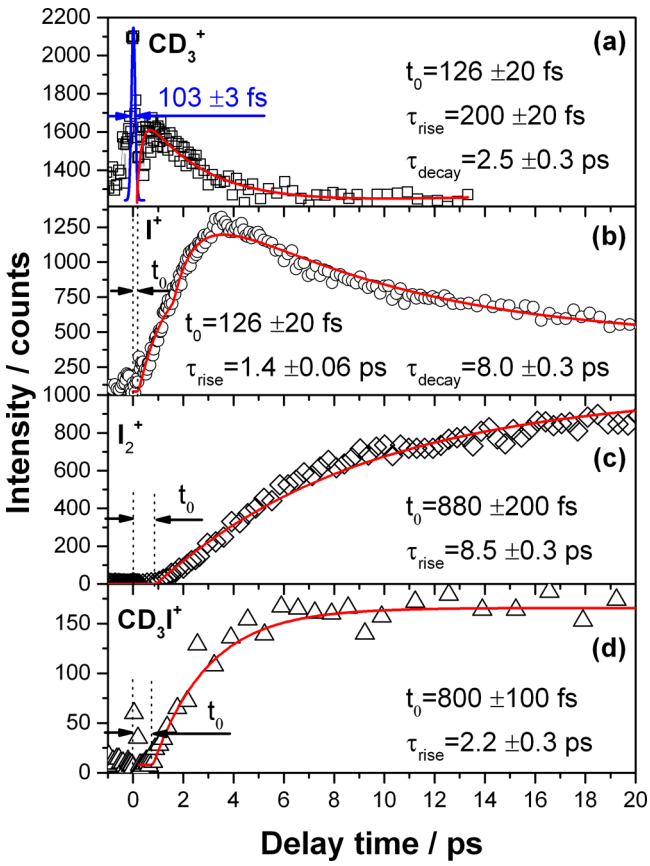

Figure 3. Transient spectra obtained by monitoring the intensity of (a) CD_3^+, (b) I^+, (c) I_2^+, and (d) CD_3I^+ peaks as a function of pump−probe time delay. The open symbols represent the experimental data, while the solid blue and red curves are the best fits of the experimental data (see the text for details). The minimum appearance time, i.e., t_0, of all species as well as the rise and decay time constants, i.e., τ_{rise} and τ_{decay}, are obtained from the fits. All transients are recorded in a single color (266 nm) pump−probe experiment with a 25 mW/cm^2 pump and 300 mW/cm^2 probe laser power after the surface was exposed for at least 250 s to the pump and probe laser radiation to passivate the surfaces (see Figure 2 and the text for details).

The initial coherent delay (t_0) of 126 ± 20 fs observed in Figure 3a,b represents the minimum time needed for the liberation of the CD_3^+ and I^+ fragments from the molecular force field and from the force field of the surface. The minimum dissociation and liberation time is strongly influenced by the adsorption geometry of the molecule on the surface.[39,41,44] In the case of methyl iodide adsorbed on MgO(100) thin films, a minimum dissociation time of 170 fs was measured by monitoring the ultrafast evolution of CD_3^+, because the molecules are adsorbed with the methyl group facing the surface and the I atom oriented toward the gas phase. In contrast, gas-phase investigations revealed a dissociation time of 120 fs for CH_3I through the $^3Q_0$ state,[45] which is the strongest optically allowed transition between the ground state and A-band. Therefore, the minimum dissociation

https://doi.org/10.1021/acs.jpclett.2c02294
J. Phys. Chem. Lett. 2022, 13, 9759−9765

and liberation time of 126 ± 20 fs measured in this experiment for both fragments suggest that both CD_3^+ and I^+ can be directly released in the gas phase without interacting with the adjacent molecules or the surface, indicating that molecular adsorption geometries with CD_3 and I facing the gas phase simultaneously exist on the amorphous cerium oxide surface.

The rise time constant, which is attributed to the average lifetime of all trajectories leading from the A-band excitation to the release of fragments[41] is much smaller for the CD_3^+ (τ_{rise} = 200 ± 20 fs) than for the I^+ fragment (τ_{rise} = 1.4 ± 0.06 ps). This suggests that immediately after the CD_3I dissociation, a large number of CD_3 fragments can be directly ejected into the gas phase while a large number of I fragments interact with the surface and adjacent molecules. In addition, the CD_3^+ rise time constant measured in this investigation is much shorter than the CD_3^+ rise time constant, i.e., 680 fs, measured in the case of CD_3I photodissociation on MgO(100) thin films, when the CD_3I molecule is adsorbed with the methyl group facing the surface, again supporting the fast ejection into the gas phase of the CD_3 fragments in the present investigation. Although various molecular adsorption geometries are possible, most of the CD_3I molecules are adsorbed with the I atom facing the cerium oxide surface and the CD_3 group oriented toward the gas phase.

The decay observed in the transient signals of CD_3^+ and I^+ displayed in Figure 3a,b suggests that these intermediate species are further involved in surface reactions. Indeed, the decay time constant of CD_3^+ (τ_{decay} = 2.5 ± 0.3 ps) matches the rise time constant of the CD_3I^+ molecule (τ_{rise} = 2.2 ± 0.3 ps), indicating that the CD_3 fragments are consumed to reform the parent molecule. Moreover, the decay time constant of I^+ (τ_{decay} = 8.0 ± 0.3 ps) matches the rise time constant of the I_2^+ molecule (τ_{rise} = 8.5 ± 0.3 ps), indicating that the I atoms are consumed to form I_2. Thus, the CD_3^+ and I^+ transient signals follow the same trend in Figure 3a,b because both species are reaction intermediates that are formed and subsequently consumed to produce CD_3I and I_2.

The background signal in Figure 3a between the 0 and 1200 counts and Figure 3b between the 0 and 1000 counts that do not present a time dependence can be attributed to dissociative electron attachment or excitation of the parent molecule into cationic dissociative states by a single laser pulse. The ion fragments produced by the pump laser pulse or the probe laser pulse alone do not affect the time-dependent pump−probe signal and do not influence the dynamics of the neutral species that are investigated in this work.

The minimum formation time (t_0) of both CD_3I and I_2 molecules is longer than 800 fs (cf. Figure 3c,d), although the CD_3 and I fragments are available at the surface 126 fs after the initial excitation of the pump laser pulse. Furthermore, CD_3I is reformed at a steady rate only after a pump−probe time delay of about 5 ps, while I_2 is formed at a steady rate only after a time delay of about 20 ps (cf. Figure 3c,d). The delayed formation of CD_3I and I_2 can be linked to the diffusion and thermalization time of the CD_3 and I fragments immediately after the dissociation of CD_3I.

To obtain further insights into the dynamics of the intermediate species, the profiles of CD_3^+ and I^+ mass peaks during the ultrafast surface reaction are monitored. Figure 4 displays a contour map in which the CD_3^+ and I^+ mass peak intensities are plotted as a function of the TOF and pump−probe time delay. The contour maps of CD_3I^+ and I_2^+ are provided in Figure S6. The fast edge of the CD_3^+ peak in

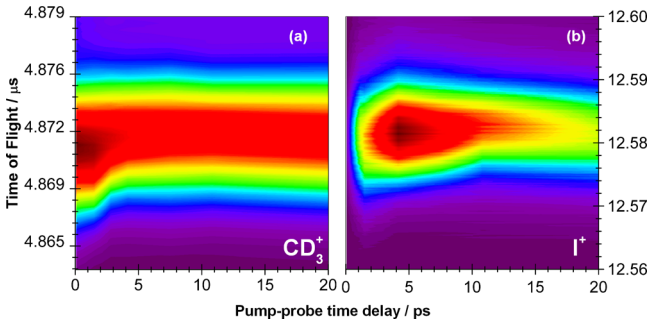

Figure 4. Contour map of (a) CD_3^+ and (b) I^+ intensities as a function of TOF and the pump−probe time delay. The mass spectra are recorded at 25 mW/cm^2 with a 266 nm pump laser beam and 300 mW/cm^2 with a 266 nm probe laser beam. The signal intensity is color-coded from purple (0%) to red (100%).

Figure 4a indicates that CD_3^+ has the shortest TOF immediately after CD_3I photodissociation (t_0 = 126 fs). Subsequently, the fast edge of the CD_3^+ peak gradually shifts to a longer TOF until a pump−probe time delay of about 4 ps and afterward does not shift. The slow edge of the CD_3^+ peak does not present a significant shift as the pump−probe time delay is varied. Figure 4b indicates that the I^+ fragment has the shortest TOF at about 1.2 ps. Subsequently, the fast edge of the I^+ peak gradually shifts to a longer TOF as the pump−probe time delay is increased to about 11 ps. At time delays longer than 11 ps, the fast edge of the I^+ fragment stays constant. The slow edge of the I^+ peak shifts to a longer TOF between 1 and 4.1 ps. After 4.1 ps, the slow edge of the I^+ peak gradually shifts to a shorter TOF as the pump−probe time delay increases.

The shift of the fast edges of the CD_3^+ and I^+ mass peaks toward a longer TOF indicates that a large fraction of these fragments is released with an excess of kinetic energy, which is lost through the interaction with the neighboring molecules or surface. The light CD_3^+ fragment and the heavy I^+ atom lose their excess kinetic energy within 4 and 11 ps, respectively. Therefore, the delayed formation of the CD_3I and I_2 is clearly linked to the thermalization of CD_3 and I, because the rates at which the products are formed increase as the excess kinetic energies of the CD_3 and I intermediates decrease. The minimum formation time (t_0) of CD_3I and I_2 can be attributed to the diffusion and a partial thermalization of the intermediates at the surface. Consequently, the CD_3I^+ and I_2^+ transient signals (cf. Figure 3c,d) follow the same trend, because these species are the final products, which are formed only after the intermediate species, CD_3 and I, lose the excess translational energy released from photodissociation.

The shift of the slow edge of the I^+ peak to longer and back to shorter TOFs during the reaction (cf. Figure 4b) can be attributed to an adsorption geometry of the methyl iodide molecule with the iodine atom facing the surface. In this case, the photodissociation of CD_3I would lead to an ejection of the I atom toward the surface. However, the pump−probe time delay of 4.1 ps at which the longest TOF of the I atom is observed (cf. Figure 4b) cannot be explained by a simple elastic interaction between the I atom and the surface, because in this case the longest TOF would be closer to ZTD. Therefore, the long TOF of the I atom at the pump−probe time delay of 4.1 ps can be attributed to an inelastic interaction of the I atom and the surface, presumably an interaction of the

https://doi.org/10.1021/acs.jpclett.2c02294
J. Phys. Chem. Lett. 2022, 13, 9759−9765

I atom and the trapped CD_3 and I fragments at the surface (see Figure 2 and the discussion above).

Power dependence measurements are performed to obtain further insights into the detection of the intermediate species and final products (see Section 6 of the Supporting Information). Probe laser power-dependent measurements indicate that the ionization of the CD_3 and I occurs after the CD_3I molecule is dissociated, because a combined energy of three photons at 266 nm (3 × 4.66 eV = 13.95 eV) is necessary for ionization, which is above the ionization potentials of CD_3 $\left(IP_{CD_3} = 9.83\ eV\right)$[46] and I $(IP_I = 10.43\ eV)$.[47] In contrast, a combined energy of two photons at 266 nm (2 × 4.66 eV = 9.32 eV) is necessary for the ionization of I_2 and CD_3I. The combined energy of two probe photons is below the ionization potential of CD_3I $\left(IP_{CD_3I} = 9.53\ eV\right)$, which indicates that the molecule is formed in an excited state, presumably an excited vibrational state of the X^1A_1 electronic state of CD_3I. The I_2 molecule might also be formed in an excited state although the ionization potential of $I_2\left(IP_{I_2} = 9.29\ eV\right)$ is just below the combined energy of two probe photons. A similar study demonstrated that the bimolecular reaction of I atoms produced by the photolysis of methyl iodide on a MgO surface leads to the formation of I_2 into the B excited state.[37]

In conclusion, this investigation provides rich physical insights on how an amorphous surface affects the dynamics of a heterogeneous photoinduced reaction and demonstrates that a priori information about the surface structure and molecular adsorption geometry are not a prerequisite to decipher the ultrafast molecular dynamics of complex photoinduced surface chemical reactions. As a model system, the ultrafast photoinduced reaction dynamics of methyl iodide adsorbed on a cerium oxide film has been investigated by an experimental technique that combines pump−probe spectroscopy with surface mass spectrometry. It was found that a fraction of the CD_3I molecules is strongly bound (chemisorbed) on low coordinated Ce atoms, and these molecules are not directly involved in the photoinduced reaction. In addition, a fraction of the first radicals that are produced via A-band excitation of CD_3I is trapped at the surface to further passivate the cerium oxide surface. Subsequently, the photoinduced reaction dynamics of CD_3I is studied on the amorphous cerium oxide film passivated with CD_3I, CD_3, and I. The minimum detection time of both CD_3^+ and I^+ fragments is 126 fs, which is very close to the gas-phase A-band dissociation time of methyl iodide. This reveals that a fraction of both fragments can be released in the gas phase without interacting with the adjacent molecules or the surface, indicating that CD_3I adsorption geometries with either CD_3 or I facing the gas phase exist. However, the rise time constant of CD_3^+, which is much smaller than the rise time constant of I^+ reveals that most of the CD_3I molecules are adsorbed with the I atom facing the surface. The CD_3 and I fragments are not produced at a steady rate because they are consumed to form molecular iodine and reform the parent molecule. The delayed formation of the CD_3I and I_2 molecules is linked to the loss of CD_3 and I translation energy, as revealed by an experiment in which the intensity of the CD_3^+ and I^+ mass peaks is monitored as a function of TOF and pump−probe time delay. Power dependence measurements show that both CD_3 and I are detected only after the CD_3I molecule is fully dissociated, while the parent molecule is reformed in an excited state, because the combined energy of the probe photons is less than the ionization potential of methyl iodide. This type of experiment can provide rich physical insights into a variety of heterogeneous reactions with high technological and industrial importance, for instance, catalytic reactions.

■ ASSOCIATED CONTENT

Supporting Information

The Supporting Information is available free of charge at https://pubs.acs.org/doi/10.1021/acs.jpclett.2c02294.

Additional experimental details, surface preparation and characterization, TPD investigations, and power dependence measurements (PDF)

■ AUTHOR INFORMATION

Corresponding Author

Mihai E. Vaida − *Department of Physics, University of Central Florida, Orlando, Florida 32816, United States; Renewable Energy and Chemical Transformations Cluster, University of Central Florida, Orlando, Florida 32816, United States;* orcid.org/0000-0002-2017-7757; Phone: +1 407-823-4213; Email: mihai.vaida@ucf.edu

Authors

Md Afjal Khan Pathan − *Department of Physics, University of Central Florida, Orlando, Florida 32816, United States;* orcid.org/0000-0003-1094-290X

Aakash Gupta − *Department of Physics, University of Central Florida, Orlando, Florida 32816, United States*

Complete contact information is available at: https://pubs.acs.org/10.1021/acs.jpclett.2c02294

Notes

The authors declare no competing financial interest.

■ ACKNOWLEDGMENTS

This material is based upon work supported by the National Science Foundation under Grant No. 1943697. A.G. acknowledges financial support provided by the UCF Office of Undergraduate Research as well as by UCF through the VPR-AECR program.

■ REFERENCES

(1) Ning, Z.; Polanyi, J. C. Surface Aligned Reaction. *J. Chem. Phys.* **2012**, *137*, 091706.

(2) Timm, M. J.; Leung, L.; Anggara, K.; Polanyi, J. C. Direct Observation of Knock on Reaction with Umbrella Inversion Arising from Zero-Impact-Parameter Collision at a Surface. *Comm. Chem.* **2021**, *4*, 14.

(3) Zallen, R.*The Physics of Amorphous Solids*; John Wiley & Sons, 2008.

(4) Yoon, C.; Cocke, D. L. Potential of Amorphous Materials as Catalysts. *J. Non Cryst. Solids* **1986**, *79*, 217−245.

(5) Montini, T.; Melchionna, M.; Monai, M.; Fornasiero, P. Fundamentals and Catalytic Applications of CeO_2-Based Materials. *Chem. Rev.* **2016**, *116*, 5987−6041.

(6) Mullins, D. R. The Surface Chemistry of Cerium Oxide. *Surf. Sci. Rep.* **2015**, *70*, 42−85.

(7) Riley, S. J.; Wilson, K. R. Excited Fragments from Excited Molecules: Energy Partitioning in the Photodissociation of Alkyl Iodides. *Faraday Discuss.* **1972**, *53*, 132−146.

(8) Sparks, R. K.; Shobatake, K.; Carlson, L. R.; Lee, Y. T. Photofragmentation of CH_3I: Vibrational Distribution of the CH_3 Fragment. *J. Chem. Phys.* **1981**, *75*, 3838−3846.
(9) Chandler, D. W.; Thoman, J. W.; Janssen, M. H. M.; Parker, D. H. Photofragment Imaging: The 266 nm Photodissociation of CH_3I. *Chem. Phys. Lett.* **1989**, *156*, 151−158.
(10) Hertz, R. A.; Syage, J. A. Detection of the Perpendicular ã State Transitions of CH_3I by Imaging of Photofragment Angle-Velocity Distributions. *J. Chem. Phys.* **1994**, *100*, 9265−9268.
(11) Li, G.; Hwang, H. J.; Jung, H. C. High Resolution Kinetic Energy by Long Time-Delayed Core-Sampling Photofragment Translational Spectroscopy. *Rev. Sci. Instrum.* **2005**, *76*, 023105.
(12) Li, G.; Hwang, H. J. State-to-State Correlated Study of CD_3I Photodissociation at 266 and 304 nm. *J. Chem. Phys.* **2006**, *124*, 244306.
(13) Khundkar, L. R.; Zewail, A. H. Picosecond MPI Mass Spectrometry of CH_3I in the Process of Dissociation. *Chem. Phys. Lett.* **1987**, *142*, 426−432.
(14) Shapiro, M.; Bersohn, R. Vibrational Energy Distribution of the CH_3 Radical Photodissociated from CH_3I. *J. Chem. Phys.* **1980**, *73*, 3810−3817.
(15) Amatatsu, Y.; Morokuma, K.; Yabushita, S. Ab Initio Potential Energy Surfaces and Trajectory Studies of A-Band Photodissociation Dynamics: $CH_3I^* \rightarrow CH_3+I$ and CH_3+I^*. *J. Chem. Phys.* **1991**, *94*, 4858−4876.
(16) Johnson, B. R.; Kinsey, J. L.; Shapiro, M. A Three-Mode Large-Amplitude Model for the Ground Electronic State of CH_3I. *J. Chem. Phys.* **1988**, *88*, 3147−3158.
(17) Lee, S. Y.; Heller, E. J. Exact Time-Dependent Wave Packet Propagation: Application to the Photodissociation of Methyl Iodide. *J. Chem. Phys.* **1982**, *76*, 3035−3044.
(18) Guo, H.; Lao, K. Q.; Schatz, G. C.; Hammerich, A. D. Quantum Nonadiabatic Effects in the Photodissociation of Vibrationally Excited CH_3I. *J. Chem. Phys.* **1991**, *94*, 6562−6568.
(19) Guo, H.; Schatz, G. C. Time-Dependent Dynamics of Methyl Iodide Photodissociation in the First Continuum. *J. Chem. Phys.* **1990**, *93*, 393−402.
(20) Alekseyev, A. B.; Liebermann, H.-P.; Buenker, R. J.; Yurchenko, S. N. An Ab Initio Study of the CH_3I Photodissociation. I. Potential Energy Surfaces. *J. Chem. Phys.* **2007**, *126*, 234102.
(21) Alekseyev, A. B.; Liebermann, H.-P.; Buenker, R. J. An Ab Initio Study of the CH_3I Photodissociation. II. Transition Moments and Vibrational State Control of the I* Quantum Yields. *J. Chem. Phys.* **2007**, *126*, 234103-1−234103-11.
(22) Cheng, P. Y.; Zhong, D.; Zewail, A. H. Femtosecond Real-Time Probing of Reactions. XXI. Direct Observation of Transition-State Dynamics and Structure in Charge-Transfer Reactions. *J. Chem. Phys.* **1996**, *105*, 6216−6248.
(23) Zhong, D.; Zewail, A. H. Femtosecond Real-Time Probing of Reactions. 23. Studies of Temporal, Velocity, Angular, and State Dynamics from Transition States to Final Products by Femtosecond-Resolved Mass Spectrometry. *J. Phys. Chem. A* **1998**, *102*, 4031−4058.
(24) de Nalda, R.; Dura, J.; Garcia-Vela, A.; Izquierdo, J. G.; Gonzalez-Vazquez, J.; Banares, L. A Detailed Experimental and Theoretical Study of the Femtosecond a-Band Photodissociation of CH_3I. *J. Chem. Phys.* **2008**, *128*, 244309−244320.
(25) Garcia-Vela, A.; de Nalda, R.; Dura, J.; Gonzalez-Vazquez, J.; Banares, L. A 4D Wave Packet Study of the CH_3I Photodissociation in the A-Band. Comparison with Femtosecond Velocity Map Imaging Experiments. *J. Chem. Phys.* **2011**, *135*, 154306.
(26) Murillo-Sanchez, M. L.; Gonzalez-Vazquez, J.; Corrales, M. E.; de Nalda, R.; Martinez-Nunez, E.; Garcia-Vela, A.; Banares, L. Femtochemistry under Scrutiny: Clocking State-Resolved Channels in the Photodissociation of CH_3I in the A-Band. *J. Chem. Phys.* **2020**, *152*, 014304.
(27) Zhou, X.-L.; Solymosi, F.; Blass, P.; Cannon, K.; White, J. Interactions of Methyl Halides (Cl, Br and I) with Ag (111). *Surf. Sci.* **1989**, *219*, 294−316.
(28) Vaida, M. E.; Tchitnga, R.; Bernhardt, T. M. Femtosecond Time-Resolved Photodissociation Dynamics of Methyl Halide Molecules on Ultrathin Gold Films. *Beilstein J. Nanotechnol.* **2011**, *2*, 618−627.
(29) Srivastava, A.; Osgood, R. M. State-Resolved Dynamics of 248 nm Methyl-Iodide Fragmentation on GaAs(110). *J. Chem. Phys.* **2003**, *119*, 10298−10306.
(30) Trentelman, K. A.; Fairbrother, H.; Stair, P. C.; Strupp, P. G.; Weitz, E. A Photofragment Spectrometer for Studying Photodissociation of Molecules Adsorbed on Surfaces: The 257-nm Photolysis of CD_3I on Mgo(100). *J. Vac. Sci. Technol. A* **1991**, *9*, 1820−1822.
(31) McCarthy, M. I.; Gerber, R. B.; Trentelman, K. A.; Strupp, P.; Fairbrother, D. H.; Stair, P. C.; Weitz, E. Photodissociation Dynamics of CH_3I Adsorbed on MgO(100): Theory and Experiment. *J. Chem. Phys.* **1992**, *97*, 5168−5176.
(32) Briggman, K. A.; Stair, P. C.; Weitz, E. Surface Residence Time Measurements of Transient Methyl Radicals. *Chem. Phys. Lett.* **2001**, *334*, 1−6.
(33) Guo, H.; Schatz, G. C. A Mechanism for the Quenching of I* in Photodissociation of Methyl Iodide Adsorbed on a Mgo Surface. *Chem. Phys. Lett.* **1991**, *184*, 245−250.
(34) Fang, J. Y.; Guo, H. Multiconfiguration Time-Dependent Hartree Studies of the CH_3I/MgO Photodissociation Dynamics. *J. Chem. Phys.* **1994**, *101*, 5831−5840.
(35) Jensen, E. T. Excitation and Quenching Mechanisms in the near-UV Photodissociation of CH_3Br and CH_3Cl Adsorbed on D_2O or CH_3OH on Cu(110). *Phys. Chem. Chem. Phys.* **2015**, *17*, 9173−9185.
(36) DeSimone, A. J.; Olanrewaju, B. O.; Grieves, G. A.; Orlando, T. M. Photodissociation of Methyl Iodide Adsorbed on Low-Temperature Amorphous Ice Surfaces. *J. Chem. Phys.* **2013**, *138*, 084703.
(37) Vaida, M. E.; Bernhardt, T. M. Surface-Aligned Femtochemistry: Real-Time Dynamics of Photoinduced I_2 Formation from CD_3I on MgO(100). *ChemPhysChem* **2010**, *11*, 804−807.
(38) Vaida, M. E.; Bernhardt, T. M.Surface-Aligned Femtochemistry: Molecular Reaction Dynamics on Oxide Surfaces. In *Ultrafast Phenomena in Molecular Sciences: Femtosecond Physics and Chemistry*; de Nalda, R., Bañares, L., Eds.; Springer International Publishing, 2014; pp 231−261.
(39) Vaida, M. E.; Bernhardt, T. M. Surface-Aligned Femtochemistry: Photoinduced Reaction Dynamics of CH_3I and CH_3Br on MgO(100). *Faraday Discuss.* **2012**, *157*, 437−449.
(40) Vaida, M. E.; Bernhardt, T. M. Surface Pump-Probe Femtosecond-Laser Mass Spectrometry: Time-, Mass-, and Velocity-Resolved Detection of Surface Reaction Dynamics. *Rev. Sci. Instrum.* **2010**, *81*, 104103−104112.
(41) Vaida, M. E.; Hindelang, P. E.; Bernhardt, T. M. Femtosecond Real-Time Probing of Transition State Dynamics in a Surface Photoreaction: Methyl Desorption from CH_3I on MgO(100). *J. Chem. Phys.* **2008**, *129*, 011105.
(42) Vaida, M. E.; Rawal, T. B.; Bernhardt, T. M.; Marsh, B. M.; Rahman, T. S.; Leone, S. R. Nonmetal-to-Metal Transition of Magnesia Supported Au Clusters Affects the Ultrafast Dissociation Dynamics of Adsorbed CH_3Br Molecules. *J. Phys. Chem. Lett.* **2022**, *13*, 4747−4753.
(43) Rulliere, C.*Femtosecond Laser Pulses*; Springer, 2005.
(44) Vaida, M. E.; Gleitsmann, T.; Tchitnga, R.; Bernhardt, T. M. Femtosecond-Laser Photoemission and Photodesorption from Magnesia Supported Gold Clusters. *Phys. Status Solidi B* **2010**, *247*, 1139−1146.
(45) de Nalda, R.; Izquierdo, J. G.; Dura, J.; Banares, L. Femtosecond Multichannel Photodissociation Dynamics of CH_3I from the a Band by Velocity Map Imaging. *J. Chem. Phys.* **2007**, *126*, 021101−021104.
(46) Chupka, W. A.; Lifshitz, C. Photoionization of CH_3; Heat of Formation of CH_2. *J. Chem. Phys.* **1968**, *48*, 1109−1115.

https://doi.org/10.1021/acs.jpclett.2c02294
J. Phys. Chem. Lett. 2022, 13, 9759−9765

(47) Grade, M.; Rosinger, W. Correlation of Electronic Structures and Stabilities of Gaseous FeI_2, Fe_2I_2 and Fe_2I_4 Molecules, Solid FeI_2, and Iodine Adsorbed on Fe. *Surf. Sci.* **1985**, *156*, 920−929.

https://doi.org/10.1021/acs.jpclett.2c02294
J. Phys. Chem. Lett. 2022, 13, 9759−9765